CLM - P 340

TEMPERATURE AND DENSITY OF AN EXPANDING LASER PRODUCED PLASMA

by

P.T. Rumsby* and J.W.M. Paul

(Submitted for publication in Plasma Physics)

ABSTRACT

The density and temperature of an expanding laser produced carbon plasma were measured over a large range of distances by several different methods. The density of an expanding element was found to have a time dependence $n_e \propto t^{-3}$. The electron temperature of the same element was found to decay with a dependence $T_e \propto t^{-1}$ rather than the theoretical adiabatic $T_e \propto t^{-2}$. These results confirm theoretical predictions about the effect of three body recombination on the cooling of a laser produced plasma.

* Also at Dept. of Engineering Science, Oxford University

U K A E A Research Group,
Culham Laboratory,
Abingdon,
Berks.

June, 1973

C O N T E N T S

1. INTRODUCTION

When an intense pulse of light from a laser is focused onto a solid material, a hot plasma is formed. The plasma expands rapidly away from the target surface as its initial thermal energy is converted to directed energy. Clearly the parameters of the expanding plasma vary enormously with both distance and time. For an understanding of processes such as recombination and cooling it is necessary to follow an expanding volume element. This was not possible in any of the experiments reported previously as these had either good spatial resolution but operated at a fixed expansion distance (DAVID, et al., 1966; IZAWA, et al., 1969; BURNETT and SMY, 1970; KOOPMAN, 1971; and EHLER, 1973) or had poor spatial resolution and averaged over a large volume of plasma (SUKOV et al, 1967; and PACK et al, 1969). The results obtained have often been conflicting; for example, electron temperatures measured 1-2 μs after the laser pulse vary from 0.01 eV (PACK et al, 1969) to 10 eV (KOOPMAN, 1971) for similar laser power densities. The nearest approach to following an element of plasma is the work of BOLAND et al (1968). They had no experimental time resolution but they followed a particular ion species during the expansion. However the measurements of n and T_e were all near the target ($r < 5$ mm) and mostly during the laser pulse.

In order to clarify this situation we have measured, with good temporal and spatial resolution, the density and temperature of the expanding plasma out to large distances using several techniques; photon scattering, microwave interferometry and ion collecting probes. From these measurements we can follow a volume element of plasma and compare its parameters with theoretical predictions.

2. THEORETICAL EXPANSION MODEL

We first consider a fully ionized plasma expanding radially outwards from a target into vacuum with no sources or sinks for energy, density or states of ionization. We assume that the plasma was created in a short interval of time sufficiently long ago that the front boundary expands freely into vacuum at constant velocity and the whole of the plasma expands uniformly preserving a normalized density profile (shape normalized to peak density and expansion radius), (ZELDOVICH and RAIZER, 1966). This will occur for either fluid or collisionless flow provided the thermal energy density is negligible compared with the kinetic energy density.

In this situation conservation of mass requires that at a given time the expansion velocity of an element of the plasma is proportional to its radius (r) and that this velocity is independent of time (t), i.e. position of the element $r \propto t$. From this it follows that the volume of the element $V \propto r^3 \propto t^3$ and hence the number density

$$n_e = \Sigma Z_i n_i \propto r^{-3} \propto t^{-3} . \qquad \ldots (1)$$

A laser produced plasma is initially highly collisional with all collision times much shorter than the laser pulse, and this situation can persist as will be discussed below. Consequently we can treat it as a single temperature fluid. For adiabatic expansion the temperature $T \propto n_e^{\gamma-1}$ and hence from Eq. (1) $T \propto r^{-3(\gamma-1)}$ or $t^{-3(\gamma-1)}$. For a highly collisional plasma $\gamma = 5/3$, and the local

$$T_e = T_i \propto r^{-2} \quad \text{or} \quad t^{-2} . \qquad \ldots (2)$$

Thermal conduction within the collisional plasma will tend to equalize the temperatures throughout the volume of the plasma at a given time. Although this will destroy the true adiabaticity of an element of plasma, the whole plasma remains adiabatic and consequently each element within it will still expand with $T \propto t^{-2}$ or r^{-2}. We assume that there is no conduction to the target, since experimentally it is found that the expanding plasma forms a shell well separated from the debris of the target.

It is important to note that with the scaling $n \propto t^{-3}$ and $T_e \propto t^{-2}$ all particle collision times $\left(\tau \propto \frac{T_e^{\frac{3}{2}}}{n \ln \Lambda}\right)$ would remain nearly constant as the expansion proceeds. A slight increase does in fact occur because $N_{debye} (= \Lambda/9)$

changes in time as $t^{-1.5}$. Thus a laser produced plasma which expands adiabatically from a highly collisional state with $T_e = T_i$ will always remain in this state.

3. RECOMBINATION AS A LOSS OF PARTICLES

We now consider the effects of recombination on the above adiabatic model. Collisional-radiative recombination (BATES et al. 1962) can for simplicity be separated into two processes; radiative recombination (ALLEN, 1955) and three-body collisional recombination (GUREVICH and PITAEVSKII, 1964; and VESELOVSKII, 1969). These processes have recombination rates given respectively by

$$R_R = \left(\frac{dn_e}{dt}\right)_R = -\alpha_R n_e n_i \,, \qquad \ldots (3)$$

and

$$R_c = \left(\frac{dn_e}{dt}\right)_c = -\alpha_c n_e^2 n_i \,, \qquad \ldots (4)$$

where

$$\alpha_R = 2.7 \times 10^{-19} Z^2 T_e^{-\frac{3}{4}}$$

and

$$\alpha_c = 9.2 \times 10^{-39} Z^3 T_e^{-9/2} \ln\sqrt{Z^2+1}$$

with T_e in eV and n_e in m^{-3}. From these rates we deduce that three-body recombination dominates over radiative recombination for

$$n_e \gg \frac{3.10^{19} T_e^{3.75}}{Z} m^{-3} . \qquad \ldots (5)$$

With the adiabatic scaling $n_e \propto t^{-3}$ and $T_e \propto t^{-2}$ we find that

$$R_{R'} \propto t^{-4.5} \qquad \ldots (6)$$

and

$$R_c = \text{constant} \qquad \ldots (7)$$

while the density decay rate due to expansion has a dependence

$$R_E = \left(\frac{dn_e}{dt}\right)_{exp} \propto t^{-4} \ . \qquad \ldots (8)$$

Clearly, if the plasma persists for sufficient time, three-body recombination will eventually dominate.

During the formation stage of plasmas produced at low laser power densities, as in the present experiment, the initial plasma densities are high ($\sim 10^{27}$ m^{-3}) and temperatures are low (20 - 50 eV) . The condition of Eq. (5) is satisfied so that three-body recombination is more important than radiative in the initial plasma. The scaling in Eqs. (6) and (7) implies that this situation will persist throughout the expansion.

The scaling of R in Eqs. (7) and (8) shows that the fall of density due to expansion may be more important than recombination initially but that eventually three-body recombination must become dominant and lead to complete recombination of the plasma.

4. RECOMBINATION AS A SOURCE OF ENERGY

In three-body recombination the electron is initially captured into an upper excited atomic level and then it cascades down to the ground level either by radiative transitions or by transferring energy to free electrons in collision of the second kind. Since this cascade process occurs very rapidly we assume that the excitation energy is transferred immediately to radiation and to the free electrons. Three-body recombination becomes important at a time when the free electron thermal energy has usually fallen to much less than the ionization energy, e.g. $\chi_i \sim 10\text{-}100$ kT/e. In this situation a very small three-body recombination rate can lead to sufficient transfer of energy to the electrons to make a large change in the electron temperature decay rate without affecting the density decay rate. This would lead to a slower cooling rate than in the above adiabatic model. The fraction of the ionization energy given to the electrons during recombination (E^*) depends on the optical thickness and plasma parameters as discussed in section 9.

KUZNETSOV and RAIZER (1965) have treated analytically the problem of a plasma expanding into vacuum with three-body recombination and energy transfer to the electrons occurring. They conclude that two situations can occur depending on whether the parameter $\xi = \frac{2E^*}{3kT}\alpha$ is greater or less than unity at the time during expansion when the ionization rate becomes negligibly small. Here α is the degree of ionization of the recombining species and kT is the plasma thermal energy.

For low α, ξ depends mainly on T through the exponential dependence of α on T. As T decreases, ξ also decreases. As an initial plasma with low α would normally also have $\xi < 1$, it would remain in this state. For high α, α is almost independent of T and so, as T decreases ξ increases. As an initial plasma with high α would not normally also have $\xi > 1$, it would remain in this state.

The analytical calculation shows that

(i) For $\xi < 1$ (low α) the energy of recombination may slightly reduce the initial cooling from the adiabatic $T \propto t^{-2}$ but asymptotically it returns to this dependence. In this case the plasma eventually recombines completely.

(ii) For $\xi > 1$ (high α) the energy of recombination reduces the cooling dramatically from the adiabatic dependence and asymptotically it acquires the dependence $T_e \propto t^{-66/65} \sim t^{-1}$. In this case the plasma does not fully recombine, i.e. the degree of ionization becomes frozen.

MATTIOLI (1971) has carried out numerical calculations on expanding LiH plasmas taking into account three-body recombination, radiative recombination and electron impact ionization. His results are very similar, indicating a transition in the temperature dependence from $T_e \propto t^{-2}$ to $T_e \propto t^{-1}$ for a sufficiently highly ionized plasma.

Table 1 shows a comparison of the scaling of the rates for different scaling of n and T.

TABLE 1

n T	t^{-3} t^{-2}	t^{-3} t^{-1}	t^{-x} t^{-1}
R_R	$t^{-4.5}$	$t^{-5.25}$	$t^{-2x+0.75}$
R_c	t^{o}	$t^{-4.5}$	$t^{-3x+4.5}$
R_E	t^{-4}	t^{-4}	t^{-x-1}

For $T \propto t^{-1}$ and $x \geq 3$ recombination will no longer dominate as $t \to \infty$ and hence there exists the possibility of freezing α. However slowly the recombination proceeds the plasma must eventually disappear.

For the scaling $T \propto t^{-1}$ and $x \geq 3$ all collision times increase with time at least as fast as $r \propto t^{1.5}$. As the plasma tends towards a collisionless state the ions will decouple from the electrons first. When this occurs the ions will no longer receive any of the recombination energy deposited in the electrons and the ions will cool adiabatically with $T_i \propto t^{-2}$. At this time they will be collisional and for $x \geq 3$ will remain so. The electrons on the other hand can maintain $T_e \propto t^{-1}$ and eventually become collisionless if the plasma persists that long.

From the above considerations we expect to observe one of the following situations depending on the initial conditions

(a) For $R_E > R_C$ (i.e. higher T, lower n) $n \propto t^{-3}$

(i)	$\xi < 1$ (lower α),	E has negligible effect	$T \propto t^{-2}$	(A)
(ii)	$\xi > 1$ (higher α),	although R small, sufficient to affect T.	$T \propto t^{-1}$	(B)

(b) For $R_C > R_E$ (i.e. lower T, higher n) $n \propto t^{-x}$, $x > 3$

(i)	$\xi < 1$ (lower α)	E has negligible effect	$T \propto t^{-2}$	(C)
(ii)	$\xi > 1$ (higher α)	E has effect	$T \propto t^{-1}$	(D)

During the expansion the plasma may change from one to another of the above but some possibilities can be excluded by scaling etc.

(i) ξ cannot change so $A, C \not\rightleftarrows B, D$

(ii) $C \not\rightarrow A$ from Eqs. (7) and (8).

(iii) $B \not\rightarrow D$ from Table I.

5. EXPERIMENT

The expanding plasma plume was formed by focusing a 37 MW 20 ns pulse from a ruby laser down to a power density of 7×10^{14} watts m^{-2} on a carbon plate target in a vacuum (2×10^{-6} torr). The four different techniques described below have yielded measurements of the plasma electron density over the range of distances from the target $r = 5$ mm to 1.3 m and electron temperature over the range $r = 20$ mm to 140 mm. The experimental arrangements are shown in Figs. 1 and 2.

Plasma electron densities were measured for $r = 5$ mm to 1.3 m by using negatively biased ion collecting probes (ASHBY, 1965). The instantaneous current to the probe is proportional to $AZn_i v$ or $An_e v$, where A is the probe aperture area, Z is the ion charge and v the ion directed velocity towards the probe. A knowledge of v, obtained from time-of-flight measurements, enables values of n_e to be obtained for any given r.

For $r = 30$ mm to 140 mm, plasma electron densities and temperatures were measured using 4 mm microwave probes (HARTWIG, 1967), in conjunction with an interferometer circuit. The expanding plasma was allowed to flow through the gap between two quartz dielectric rod antennae. Two probes were used with antenna gaps of 12 mm and 34 mm and antenna sizes such that they had spatial resolutions of 5 x 5 mm and 9 x 9 mm respectively both parallel and perpendicular to the plasma flow. The larger probe was used only at expansion distances greater than 90 mm. With a 100 ohm detector load the response time of the system was estimated to be about 10 ns. By monitoring the interferometer phase shift, electron densities between 1×10^{18} and 5×10^{19} m^{-3} could be measured. Simultaneous measurements of the phase shift, the transmitted and the reflected powers enabled the attenuation coefficient and hence the effective electron-ion collision frequency to be determined at any position. From these measurements values of the local electron temperature were obtained.

For $r = 20$ mm to 50 mm densities and temperatures were measured by the technique of photon scattering using ruby laser light. The second, probing laser beam (110 MW, 20 ns), was focused to 2 mm diameter in the plasma. A 1 mm diameter region was observed at a scattering angle of 135^0 and the scattered light was spectrally resolved by rotating a narrow band (0.25 nm) interference filter centred at 694.3 nm.

The expanding plasma was examined at different distances from the target surface without disturbing the scattering optics by moving the carbon rod target and focusing lens together along the direction of the first laser beam. The scattering technique could be used over a limited range $20\,mm < r < 50\,mm$. For $r > 50\,mm$ the scattered signal was too small due to the low plasma density, while for $r < 20\,mm$ the stray light from the hot target surface was prohibitively large.

An estimate of the electron temperature occurring very near the target surface during the laser pulse was made by comparing the intensities of two CV lines at 4.027nm and 3.498 nm using a grazing incidence spectrograph (GRIEM, 1964). The slit was aligned along the target normal and the aperture was such that the spectrograph registered time and space integrated light from the region $0 < r < 2\,mm$.

6. ELECTRON DENSITY RESULTS

Using the ion collecting probe, measurements were made of the variation of the local electron density with time at many positions along the target normal. This data was converted into spatial profiles at various times after the laser pulse. Some of the profiles obtained are shown in Fig.3.

The expanding plasma can be seen to consist of two components:

(1) A relatively thin shell of plasma which expands rapidly away from the target with constant velocity $v \sim 100\,km\,s^{-1}$; and

(2) An almost stationary dense core which recombines rapidly without moving beyond $r \sim 12$ mm.

The microwave probe gave measurements of electron densities agreeing to within 30% with those of Fig.3 for the leading edge and just behind the peak density of the shell. For later times discrepancies of up to a factor of three arose, probably due to plasma being trapped between the probe antennae.

In order to determine the true scaling of the density decay it is necessary to follow in time a single element of expanding plasma, as discussed earlier. We choose to follow the peaks of the shell density profiles. This corresponds to following a single plasma element provided that the normalised profile is maintained throughout the expansion. This is indeed so as discussed below. Fig.4 shows the variation in time of the peak shell density over the whole range of measurements made with the charge collector probe. The density falls exactly as t^{-3} over six orders of magnitude showing that the density decay rate due to recombination is negligibly small compared with that due to expansion.

Close examination of the profiles of Fig.3 shows that the normalised density profile is indeed preserved throughout expansion as assumed. In Fig.4 the areas under each of the profiles is shown to have a t^{-2} dependence for the range of measurements. Thus, together with the t^{-3} dependence of the peak density, implies that the shell width increases linearly with time and that the plasma expansion velocity at a given time increases linearly from the back to the front of the shell. The normalised density profile is therefore preserved. (Such a velocity profile has been predicted previously (FADER, 1968) in a computation of the expansion of a laser produced plasma.) The basic assumptions of the expansion model presented in Section 2 are valid in this experiment, i.e. constant normalised density profile with velocity of element independent of time but at a given time velocity proportional to radius and no sources or sinks.

7. ELECTRON TEMPERATURE RESULTS

The microwave probes have yielded measurements of the effective collision frequency at various positions in the leading edge and at the peak density in the expanding shell. Fig.5 shows the time variation of the collision frequencies measured at the peak of the shell, i.e. following a volume element. The error bars do not reflect shot-to-shot variation which is small but indicate uncertainties in the absorption measurement. These errors increase at later times as the absorption coefficient becomes smaller.

Over the range of measurements the plasma can be seem to be highly collisional while the decrease in the collision frequency with time suggests that there has been some departure from the adiabatic temperature scaling which should maintain the collision frequency constant.

For times earlier than 0.6 μs the peak shell density exceeded the cut-off density for 4 mm microwaves and collision frequency measurements were made in the leading edge of the shell. Typical errors in these cases are similar to those shown in Fig.5 at times greater than 1.2 μs. These are not due to uncertainties in the absorption measurement so much as to uncertainties in the density measurement caused by the large gradient in the front of the shell.

From the local measurements of collision frequency and electron density, values of electron temperature were calculated using the expression (HEALD and WHARTON, 1965)

$$\nu_{ei} = \frac{2.9 \times 10^{-12}\, Z\, n_e \, \ell n\, \Lambda_{eff}}{T_e^{\frac{3}{2}}}$$

where

$$\Lambda_{eff} = \frac{6.2 \times 10^{4}\ T_e^{\frac{3}{2}}}{Zf}$$

with n_e in m^{-3}, T_e in eV and f, the frequency of the microwaves, in GHz.

Fig.6 shows the variation of this measured electron temperature with time and this is very close to a t^{-1} dependence. Points marked with open circles correspond to measurements made at the peak of the shell. Triangles indicate measurements made in the leading edge of the shell for times when $n_{peak} > n_{crit}$. These were all made at a fixed density of $\frac{1}{3} n_{crit} = 2 \times 10^{19}\ m^{-3}$. Squares refer to measurements made in the leading edge but at a time when $n_{peak} < n_{crit}$ and at a density of $\frac{1}{2} n_{peak}$.

The very close agreement between the peak and leading edge measurements at 0.6, 0.7 and 0.8 μs shows that the electron temperature throughout the front half of the shell is the same at any given time. We expect the electron temperature to be uniform throughout the plasma shell at any instant during its expansion and cooling so long as $v_{th} > v_{sep}$, where v_{th} is the electron thermal velocity and v_{sep} is the difference between the expansion velocities of the front and back of the shell. This is the case in this experiment which has $v_{sep} \sim 60\text{–}70\ km\ s^{-1}$ so long as $T_e > 0.025\ eV$. This condition is valid for all the measured temperatures but, assuming $T \propto t^{-1}$, only for $t < 6\ \mu s$, i.e. $r < 0.6\ m$.

8. PHOTON SCATTERING MEASUREMENTS

The measurements of electron temperature presented in Fig.6 are obtained by a relatively indirect method and could be subject to uncertainty. We have made an unambiguous check of these results by the well established technique of scattering laser light (EVANS and KATZENSTEIN, 1969). This also yields a third measurement of density. The measurements were carried out at the peak of the shell density for $20\,\mathrm{mm} < r < 50\,\mathrm{mm}$. Fig.7 shows a typical scattered light spectrum, obtained at $r = 20\,\mathrm{mm}$, $t = 0.2\,\mu s$. Even for a scattering angle of 135°, the plasma parameters were such that the scattering parameter $\alpha = (k\lambda_D)^{-1}$ lies between 0.1 and 0.4, and the spectrum departs from a Gaussian. To analyse such results theoretical spectra were calculated and the best fit to the experimental one found by trial and error. This fitting to α and T_e allows the calculation of the density. As a check the densities were also measured by comparing the total scattered intensities with Rayleigh scattering from nitrogen at atmospheric pressure. Table 2 shows the results obtained, all at the peak density of the shell.

TABLE 2

r. mm	t µs	T_e eV	α by curve fitting	n_e m^{-3} from α	n_e m^{-3} by Rayleigh
20	0.2	0.65 ± 0.1	0.35 ± 0.1	$1.2 \pm 0.5 \times 10^{21}$	$1.2 \pm 0.2 \times 10^{21}$
30	0.3	0.4 ± 0.05	0.3 ± 0.15	$5.6 \pm 3.0 \times 10^{20}$	$5.0 \pm 0.8 \times 10^{20}$
40	0.4	0.3 ± 0.04	between 0 and 0.2	up to 3×10^{20}	$1.2 \pm 0.2 \times 10^{20}$
50	0.5	0.3 ± 0.03	0	-	$9.5 \pm 0.8 \times 10^{19}$

As the plasma expands α decreases (for $T_e \propto t^{-1}$, $\alpha \propto t^{-1}$) and the scattered spectrum approaches a gaussian form. The calculation of the density by the curve fitting method gave reasonable accuracy only for $\alpha \geq 0.3$.

The density results obtained by scattering (Rayleigh) are plotted in Fig.4 and agree to within 50% with the charge collector probe results. The t^{-3} dependence is also confirmed. The electron temperature results obtained by scattering are plotted in Fig.6 and agree to within 25% with the microwave probe results. The t^{-1} dependence is confirmed.

Finally we have the temperature measurement made at the target surface. From the ratio of the two CV lines we have estimated (GRIEM, 1964) a temperature of 30 eV assuming LTE and 40 eV assuming a coronal equilibrium.

Taking into account the temporal and spatial averaging involved in the measurements we estimate a temperature of about 40 eV occurring at a distance of a few 100 μm from the target.

9. DISCUSSION

The temperature measured close to the target surface is supported by the work of PUELL, (1970). He has developed a steady state plasma production model for massive targets from which the maximum electron temperature can be calculated. This occurs at a distance from the target roughly equal to the focal spot radius. Excellent agreement was found between this theory and experimental measurements made by Puell with carbon targets. Applying this theory to the present experiment predicts a maximum electron temperature of about 50 eV at a distance of about $r = 0.2$ mm, which agrees well with the experimental result. The theory also predicts that the electron density corresponding to this situation should be close to the critical density for the ruby laser wavelength, $\sim 2 \times 10^{27}$ m^{-3}.

Figures 4 and 6 show that at long times after the laser pulse the density and temperature within the shell are falling as $t^{-3}(r^{-3})$ and $t^{-1}(r^{-1})$ respectively. If we use these dependences to calculate the plasma parameters at $r = 0.2$ mm from the measurement at $r > 20$ mm, we find $T_e = 40 - 50$ eV and $n_e = 10^{26} - 10^{27}$ m^{-3}. This temperature value agrees closely with the measured value and with the above theoretical prediction. This implies that the t^{-1} scaling of T_e has been maintained throughout the whole expansion. The density obtained by extrapolating back to $r \sim 0.2$ mm is somewhat lower than that predicted theoretically implying that more than half of the plasma has recombined at early times. This is in accord with the observed recombining component of the plasma. Direct comparison of these results with those of BOLAND et al, (1968) for the early stages of expansion is not possible. They have $n_e \propto t^{-x}$ with $x < 3$, i.e. not 3-dimensional expansion. However x tends to 3 as r tends to 5 mm towards the end of the measurements.

We wish to check that the calculated recombination rates are in fact sufficiently low to be negligible compared with the density decay rate due to expansion at late times as experimentally observed. In order to do this we first need to determine the mean ion charge state at the peak of the expanding shell. This can be obtained from Puell's theory which derives an expression relating the ion expansion energy, the ion charge state, and the initial electron temperature,

$$E(\text{eV}) = 5(Z+1)\, T_e(\text{eV}).$$

Applying this to the peak of the shell ($v = 100\ \text{km.s}^{-1}$, $E = 625$ eV) assuming $T_e = 45$ eV gives a mean Z of 1.8 .

It is interesting to note that the maximum ion energy observed in the expanding shell ($v_{max} = 130\ \text{km.s}^{-1}$) was 1.05 keV which from the above expression gives an ion charge at the shell front of 3.7. This result is consistent with the experimental spectrographic observation of weak CV lines but no CVl lines.

Using the mean value of $Z = 1.8$ the density decay rates due to expansion, three-body recombination and radiative recombination at the shell peak at 0.5 μs ($R = 50$ mm) are respectively 5.4×10^{26}, 4.8×10^{24} and $1.0 \times 10^{22}\ \text{m}^{-3}\ \text{s}^{-1}$. As expected the two recombination rates are negligible compared with the rate due to expansion. At later times these differences become even greater because for $T_e \propto t^{-1}$ the above decay rates scale as t^{-4}, $t^{-4.5}$ and $t^{-5.25}$ respectively. On the other hand at much earlier times one might expect a situation where the three-body recombination rate approaches the density decay rate due to expansion. This is consistent with the observed loss of some fraction of the plasma at early times as discussed above.

A quantitative discussion of the recombination rates occurring at early times is complicated by two factors.

First the three-body recombination coefficient given earlier is an over-estimate at temperatures above about 1 or 2 eV since electron capture is now directly into lower levels, and secondly, electron impact ionization becomes important.

The three-body recombination rate at 0.5 μs quoted above is sufficient to account for the observed change in cooling rate from t^{-2} to t^{-1} for a value of $E^* \approx 0.2$. BATES and KINGSTON (1964) have calculated E^* for recombining hydrogen plasmas with parameters similar to those of the present experiment. For plasmas which are optically thin they find $E^* \sim 0.1$ to 0.2, while for the optically thick case $E^* \sim 0.7$ to 0.9, due to the trapping of resonance radiation.

We have calculated that the present carbon plasma is marginally optically thick to CII and CIII resonance radiation up to expansion times of a few microseconds. At later times however the plasma becomes optically thin. In this calculation we have taken into account the Doppler broadening of the lines due to the differential expansion velocities of the various plasma regions.

Thus for the carbon plasma of the present experiment we might expect to achieve $E^* \geq 0.2$ and hence satisfy the above heating requirement.

The observed scaling $n_e \propto t^{-3}$ and $T \propto t^{-1}$ implies that all collision times increase as $\tau_{coll} \propto t^{1.5}$ and, if the plasma persist for long enough, it will eventually become collisionless. From the measured parameters we expect that the ions become decoupled from the electrons early in the expansion ($r \sim 20$ mm) and thereafter cool as $T_i \propto t^{-2}$. The electrons are still collisional at the largest distance of observation $R \sim 1.3$ m.

The observations clearly show that the expansion corresponds to case B of Section 4. Thus we achieve the higher T, higher α case even with low laser power and consequently conclude that most laser produced plasmas will expand in this way. Also it is the lower density case so that longer wave length lasers with even lower initial densities will also follow this behaviour.

10. CONCLUSIONS

We have demonstrated experimentally that the density and temperature of an element of expanding plasma decrease as t^{-3} and t^{-1} respectively. The temperature scaling is modified from the expected adiabatic one $T_e \propto t^{-2}$ because three-body recombination injects energy into the electrons. This result agrees well with theoretical predictions.

ACKNOWLEDGEMENTS

The authors wish to acknowledge the encouragement and advice from Dr R.J. Bickerton and the technical assistance from Drs M. Masoud and M. Galanti.

REFERENCES

ALLEN, C.W., 'Astrophysical Quantities', Athlone Press, London (1955).

ASHBY, D.E.T.F. et al., AIAA Journal, 3, 1140 (1965).

BATES, D.R. et al., Proc. Roy. Soc., London A267, 297 (1962).

BATES, D.R. and KINGSTON, A.E., Proc. Roy. Soc., 279A, 10 (1964).

BOLAND, B.C. et al., J. Phys. B., 1, 1180 (1968).

BURNETT, N.M. and SMY, P.R., Can. J. Phys., 48, 1421 (1970).

DAVID, C. et al. IEE J. Quant. Elec., QE-2, 493 (1966).

EHLER, W., Phys. Fluids, 16, 339 (1973).

EVANS, D.E. and KATZENSTEIN, J., Rep. Prog. Phys., 32, 207 (1969).

FADER, W.J., Phys. Fluids, 11, 2200 (1968).

GRIEM, H.R., 'Plasma Spectroscopy', Chp. 13, McGraw-Hill, N.Y., (1964).

GUREVICH, A.V. and PITAEVSKII, L.P., Sov. Phys. JETP, 19, 870 (1964).

HARTWIG, H., Report No. JUL-473-PP, Julich (1967).

HEALD, M.A. and WHARTON, C.B., 'Plasma Diagnostics with Microwaves', Chp.2, Wiley, N.Y., (1965).

IZAWA, Y. et al. Japan J. Appl. Phys., 8, 965 (1969).

KOOPMAN, D.W., Phys. Fluids, 14, 1707 (1971).

KUZNETSOV, N.M. and RAIZER, Yu.P., Zh. Priklad. Mekhan. Tech. Fiz., 4, 10 (1965).

MATTIOLI, M., Plasma Phys., 13, 19 (1971).

PACK, J.L. et al., Phys. Fluids, 12, 469 (1969).

PUELL, H., Z. Naturforsch, 25a, 1807 (1970).

SUKOV, E.W. et al., Phys. Fluids, 10, 2035 (1967).

VESELOVSKII, I.S., Sov. Phys. Tech. Phys., 14, 193 (1969).

ZELDOVICH, Ya.B. and RAIZER, Yu.P. In 'Physics of Shock Waves and High-Temperature Hydrodynamic Phenomena', Academic Press, New York, (1966).

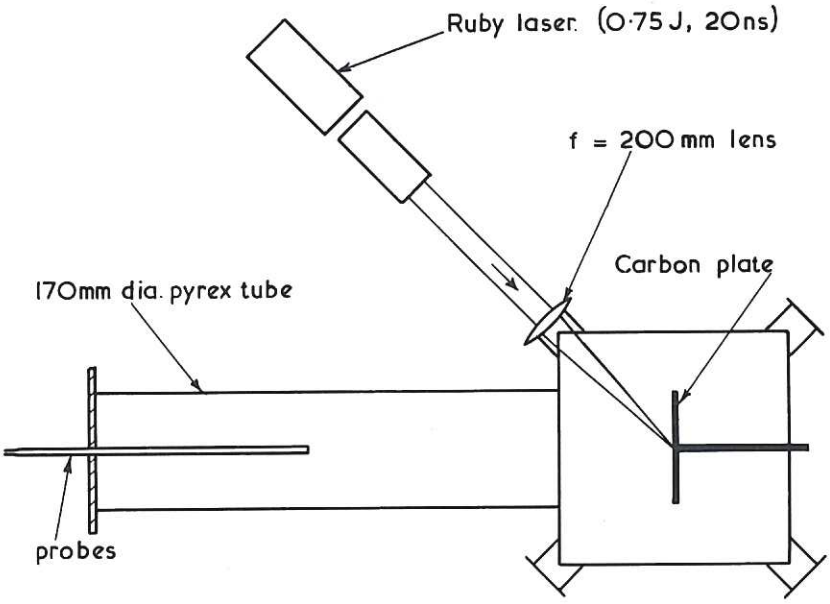

Fig.1 Experimental arrangement for charge collector and microwave probe measurements.

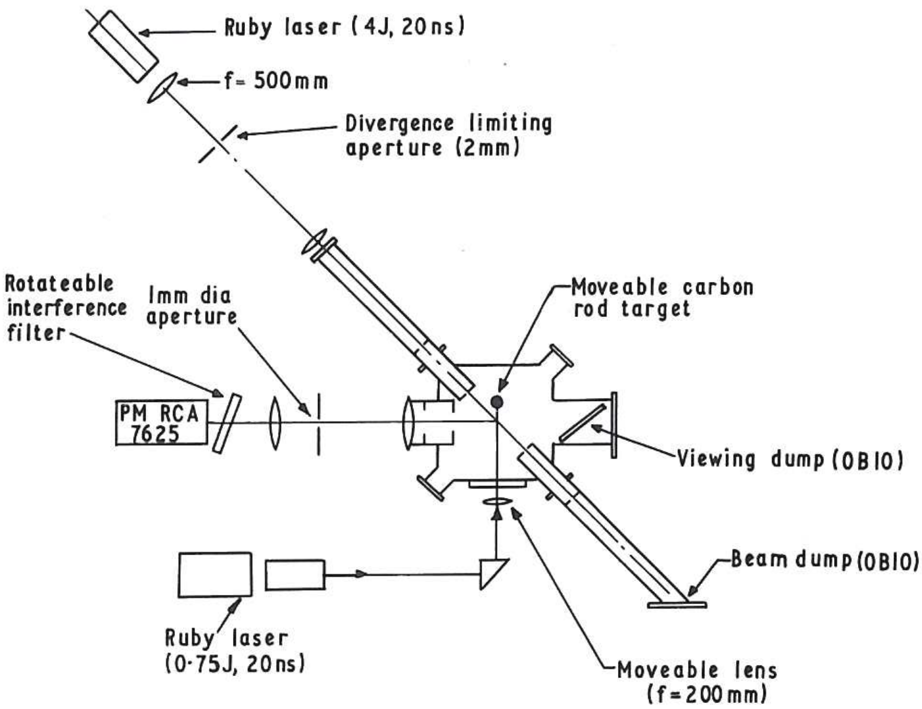

Fig.2 Experimental arrangement for laser scattering measurements.

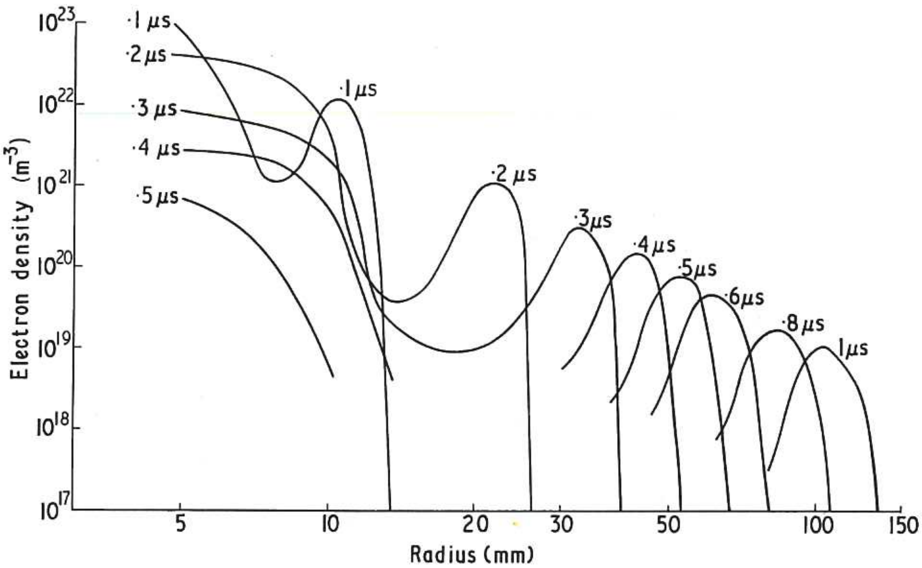

Fig.3 Electron density space profiles at various times after the laser pulse.

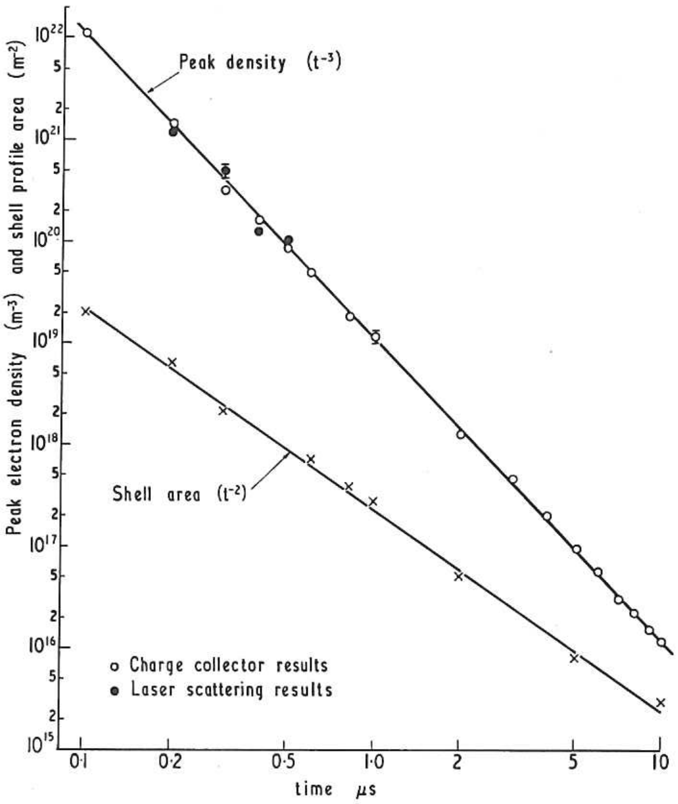

Fig.4 Variation in time of shell peak density and shell area.

CLM-P 340

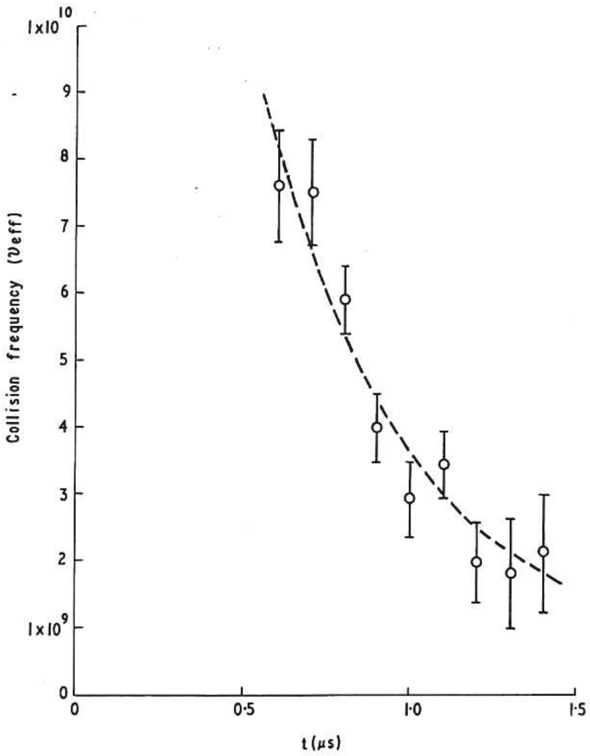

Fig.5 Variation in time of the collision frequency at the peak shell density.

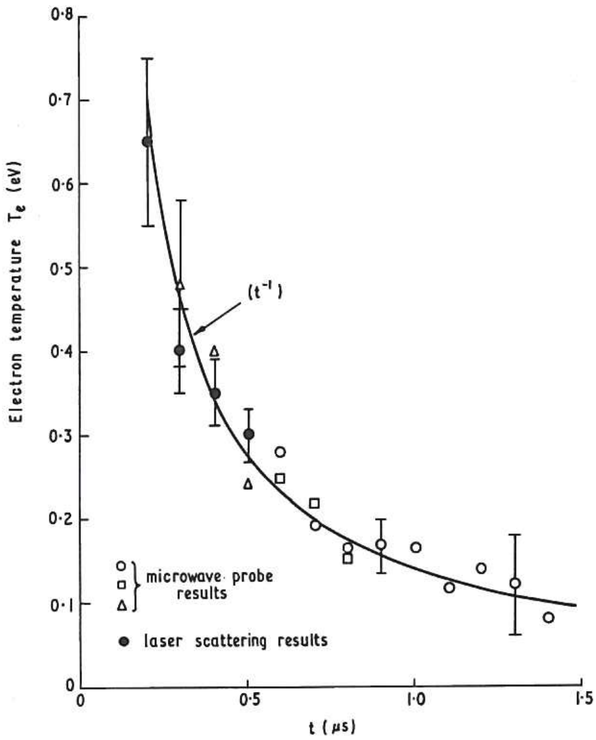

Fig.6 Shell electron temperature variation with time.

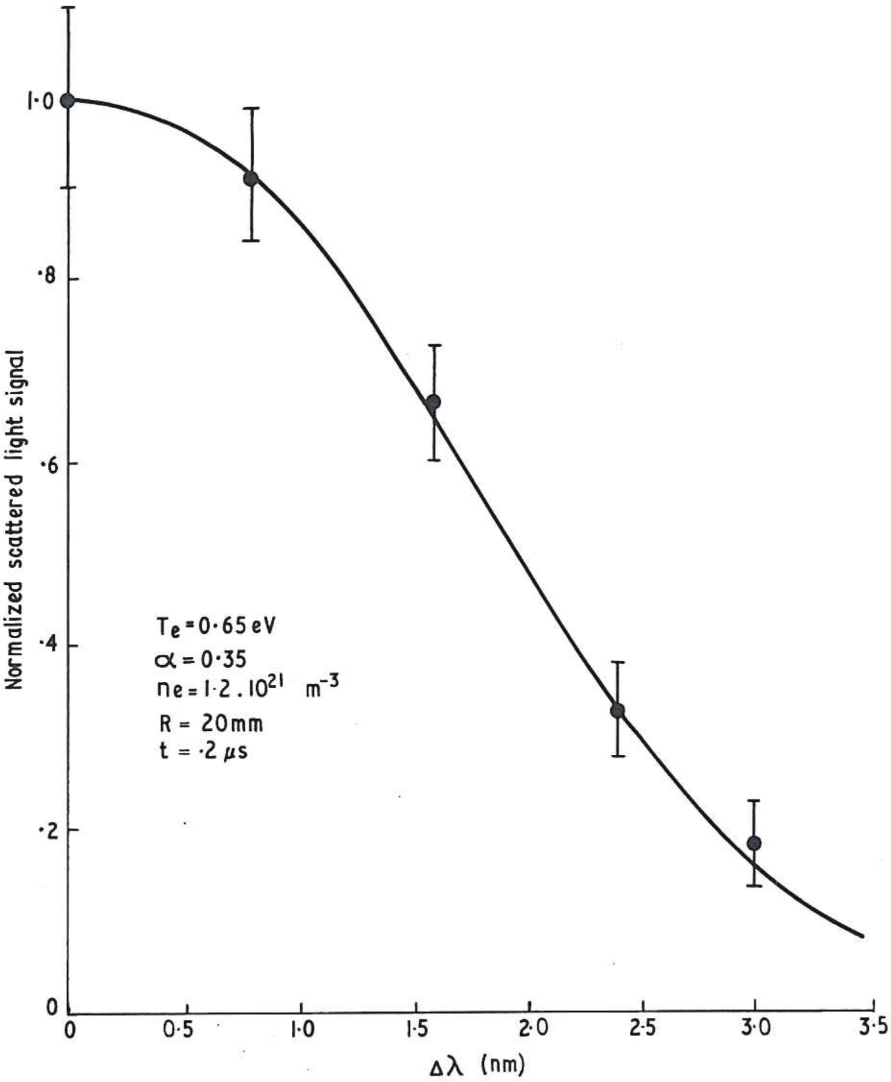

Fig.7 Typical scattered light data and best fit curve.